JOURNAL OF AGRICULTURAL AND FOOD CHEMISTRY

PVPP−Polyphenol Complexes: A Molecular Approach

BÉNÉDICTE LABORDE,[†,‡] VIRGINIE MOINE-LEDOUX,[§] TRISTAN RICHARD,[†] CÉDRIC SAUCIER,[‡] DENIS DUBOURDIEU,[‡] AND JEAN-PIERRE MONTI*[,†]

Laboratoire de Physique et Biophysique, GESVAB EA 3675, Université de Bordeaux 2, 146 rue Léo Saignat, 33076 Bordeaux Cedex, France, Faculte d′Oenologie, UMR Oenologie-Ampélologie 1219, Université de Bordeaux 2, 351 Cours de la Libération, 33405 Talence Cedex, France, and Laffort Oenologie, BP 17-33015 Bordeaux Cedex, France

In dry white wines, two different forms of instability occur: (i) substantial yellow or yellow-green deposits are observed principally due to flavonol quercetin; and (ii) protein instability leads to protein casse. Polyvinyl polypyrrolidone (PVPP) is used to adsorb phenols from beverages, and bentonite is used to eliminate heat instable protein. However, in both cases, their effects are still largely unknown. This study uses a multitechnique approach to gain a better molecular understanding of the association of polyphenol aglycones with PVPP compared to that of glucosides with PVPP. The work demonstrates, that with aglycones, three forces drive complex formation: hydrophobic interaction, H bonds, and van der Waals bonds. With glucosides, the sugar moiety removes or reduces these driving forces. Thus, if the interaction between proteins and polyphenols is responsible for haze and precipitates, as is classically assumed, PVPP could prevent quercetin sedimentation.

KEYWORDS: Interaction; polyphenols; PVPP; ESI/MS; NMR

INTRODUCTION

In white wines, various different forms of instability occur. An unusual form of instability occurs when substantial yellow or yellow-green deposits are observed during bulk or bottle storage. The deposits mainly consist of the flavonol quercetin with kaempferol and myrecetin (*1*). The presence of quercetin, kaempferol, and myrecetin at trace levels is due to extraction of their respective glucosides from grape skins and their subsequent hydrolysis (*2*). Their low aqueous solubilities ensure their sedimentation. This phenolic instability is partly due to changes in viticultural and winemaking practice, such as the use of machine-harvesting, which increases the presence of contaminant leaves, earlier bottling (3), and greater exposure of berries to the sun (*4*).

The protein instability occurring in dry white wines is still not fully understood. To prevent protein casse, bentonite is used to eliminate heat unstable protein but with the risk of an overall reduction in their organoleptic properties. Since the interactions between proteins and polyphenols are responsible for haze and precipitates (*5*−*7*), this protein casse might result from the formation of protein−polyphenol complexes, even though the polyphenol concentrations in dry white wines are low. Indeed, the improvement, by an invertase fragment, of the protein stability of such wines might be due to competition between this fragment and wine proteins with regard to polyphenols (*8*).

However, glycoside polyphenols are largely present in wines and we recently demonstrated that the association of polyphenol with peptides is better with aglycones than with glycoside polyphenols (*9*, *10*). To compare the behavior of these molecule families related to complex formation, quercetin and quercetin-3-*O*-glucoside were used as models because (i) quercetin is one of the main components of the observed deposits, and (ii) the results could be compared to those of a recent work which studied the influence of the sugar moiety of rutin on its reactivity with whey proteins (*11*).

Water-insoluble polyvinyl polypyrrolidone (PVPP) and water-soluble poly(vinylpyrrolidone) (PVP) are synthetic polymers which are used to adsorb phenols from beverages. It is thought that they interact with polyphenols via H bonds between their CO−N linkages and phenol groups (*12*). Similar interactions could explain the formation of the polyphenol−protein complex (*5*). Thus, it is reasonable to postulate that polymers and proteins behave similarly. Indeed, Siebert et al. showed that the mechanisms by which polyphenols attach to PVPP and protein are similar (*13*).

The present report investigated the use of PVPP in wines to eliminate quercetin sedimentation, explored the molecular mechanisms by which polyphenols bind to PVPP, and examined the role of glycosides in the binding process. To obtain these molecular insights, we used 1-ethyl-2-pyrrolidinone (EP) because the complexity of the PVPP molecule and its water-soluble PVP precludes such a study. Such an investigation could also

* Corresponding author. Phone: 33-(0)5-5757-1792. Fax: 33-(0)5−5757−4563. E-mail: jean-pierre.monti@physique.u-bordeaux2.fr.
[†] Laboratoire de Physique et Biophysique, GESVAB EA 3675, Université de Bordeaux 2.
[‡] Faculte d′Oenologie, UMR Oenologie-Ampélologie 1219, Université de Bordeaux 2.
[§] Laffort Oenologie.

10.1021/jf060427a CCC: $33.50
Published on Web 05/17/2006

increase our knowledge of the binding mechanisms by which polyphenols interact with proteins.

MATERIALS AND METHODS

Materials. The following reagents were purchased from commercial companies and used without treatment, except for PVPP, which was purified by heating (30 min, 100 °C) in an acid solution (12 N HCl) and washing with water to pH 7.

Water, quercetin, acetic acid, and PVPP were from Sigma (Steinheim Germany) and ethyl-pyrrolidinone (EP) was from Aldrich (Steinheim Germany). Acetonitrile and methanol were from VWR (Fontenay-sous-bois, France). Quercetin 3-*O*-β-glucopyranoside was from Extrasynthese (Genay, France).

Quercetin and Quercetin-3-*O*-glucoside in White Wines. To evaluate the action of PVPP, 10 mg/L of quercetin and quercetin-3-*O*-glucoside (concentration maxima estimated) were added to 100 mL of a white dry wine (Doisy Daëne 2003). Before addition, the initial concentrations of these molecules in the wines were measured. Then, after addition of flavonols, various concentrations of PVPP were tested as is recommended in wines (maximum: 80 g/hL) (*14*). The samples were mixed for 90 min and centrifuged. Finally, quercetin and quercetin-3-*O*-glucoside free concentrations were obtained by HPLC in supernatants (see below). Three independent measurements were made, and results are presented with means and standard deviations.

Polyphenol−PVPP Complexes in Model Solutions. *Complex Formation*. To determine the binding parameters of the polyphenol−PVPP association, various methanol solutions (100 mL) of quercetin and quercetin-3-*O*-glucoside were mixed with PVPP (10 g dL^{-1}). The samples were mixed for 90 min and then centrifuged. The free concentrations of polyphenols in supernatants were analyzed by HPLC (see below). Three independent measurements were made, and results are presented with means and standard deviations.

Binding Parameter Measurement. The binding parameters of the polyphenol−PVPP interaction were calculated by using a least-squares fitting technique to match the experimental data with a theoretical curve generated by the classical binding equation:

$$\frac{L_{\text{bound}}}{R_{\text{tot}}} = n\frac{L_{\text{free}}}{L_{\text{free}} + K_{\text{d}}}$$

where L_{bound} and L_{free} are the bound and free concentrations of polyphenol, respectively, n is the number of independent and identical binding sites, R_{tot} is the PVPP concentration, and K_{d} is the dissociation constant.

HPLC Analysis of Flavonols. The HPLC apparatus was a Thermoelectron system including an automated gradient controller, an SCM 1000 data module, P1000R pumps, an AS 1000 injector, and a UV 3000 wavelength detector. The method was described by Cheynier and Rigaud (1986). The samples were directly analyzed with a Lichrospher RP 18 column (5 μm, 4.6 cm, 250 mm) using the following gradient: solvent A, acetonitrile; solvent B, 4% acetic acid in water; initial, 10% A; 0−30 min, 10−25% A; 30−40 min, 25−40% A; 40−45 min, 40−60% A; 45−60 min, 60−100% A; flow rate, 1 mL per minute; room temperature.

The effluent was monitored by its absorbance at 365 nm. Quercetin and quercetin-3-*O*-glucoside concentrations were calculated after standardization with known concentrations of flavonols under the same experimental conditions.

Titration Experiments by NMR for Polyphenol−EP Complexes. For titration experiments, two identical 20 mM quercetin samples A and B were prepared in the solvent ($^2H_4$)-methanol (CD_3OD). In sample A, aliquots of a 1 M 1-ethyl-2-pyrrolidinone (EP) solution were added, giving different EP/quercetin molar ratios. In sample B, the same aliquots of CD_3OD were added, giving a quercetin chemical shift reference solution. During titration, it was verified that the pH did not change. Moreover, by titrating CD_3OD in a mixture of quercetin and EP, we checked that any possible effect of the solvent on the complex formation was negligible. The same protocol was used with quercetin-3-*O*-glucoside.

The chemical shift variations ($\Delta\delta_i$) derived from titration experiments were used to determine the dissociation constant (K_d), the maximum change in chemical shift ($\Delta\delta_{max}$), and the number n of EP molecules in association with polyphenols under our experimental conditions. A least-squares fitting technique matched the experimental data $\Delta\delta_i$ with a theoretical curve generated by Baxter's equation (*15*).

NMR Spectroscopy Experiments. NMR experiments were conducted on a Bruker Avance-500 NMR spectrometer. 20 mM solutions of quercetin or quercetin-3-*O*-glucoside−EP mixtures (molar ratio 1/20) in CD_3OD were used for all experiments. NMR spectra were referenced to internal trimethylsilyl-3-propionic acid-d_4-2,2,3,3 sodium salt (TMSP). TOCSY spectra were acquired with a total spin-lock mixing time of 90 ms. Off-resonance ROESY spectra were acquired with mixing pulses of 200 and 400 ms, respectively. Water suppression was accomplished by use of a WATERGATE sequence. Heteronuclear multiple bond correlation (HMBC) spectra were optimized on long-range couplings with a low-pass J-filter to suppress one-bond correlations, without any decoupling during acquisition and by using gradient pulses for selection. Data were processed with XWINNMR from Bruker SA. One-dimensional NMR spectra were used to determine the chemical shift variation in the titration experiments.

Mass Spectroscopy. Methanol mixture solutions of quercetin or quercetin-3-*O*-glucoside with EP were prepared to obtain two different polyphenol/EP molar ratios: 1/1 and 1/10, respectively. The mass spectra were acquired on a single quadrupole platform II mass spectrometer (Micromass, Waters, France) coupled with an HPLC (Agilent 1100 series). The sample (10 μL) was injected directly (without a column) into the mass spectrometer at a rate of 0.1 mL/min of methanol by using an HPLC pump. Electrospray ionization mass spectrometry detection was performed in negative ion mode with the following optimized parameters: source temperature, 120 °C; nebulizer nitrogen flow, 9 L/h; drying nitrogen flow, 220 L/h; capillary voltage, 3.5 kV; cone voltage, −30 eV. Scanning was performed from $m/z = 0$ to $m/z = 2500$ for solutions of the complexes. Resolution was set to 1 u over the scanned mass range. Pure methanol solutions of quercetin and quercetin-3-*O*-glucoside (2 mM) were examined separately under the same experimental conditions.

Molecular Modeling. To evaluate the binding between synthetic polymers and polyphenols, a pentameric structure of PVP (EP5) was built using the Hyperchem software package. Atom charges were calculated by using the AM1 semiempirical method. Molecular mechanic energies were calculated by using the MM+ force field. To obtain the most stable family, EP5 was subjected to 500 optimizations of conformational searching, using the Monte Carlo multiple minimum (MCMM) method with usage-directed searching (*16*, *17*). Torsional alkyl "backbone" angles were simultaneously varied for each MCMM step. The structures were energy-minimized by 200 steps of a steepest descent algorithm and 5000 maximum steps of a Polak−Ribiere conjugate gradient, until the energy gradient was smaller than 0.02 kcal mol^{-1}. The structures were clustered using a RMSD (root-mean-square deviation) of heavy atoms with a threshold of 0.4 Å. Then, the mean molecule representing the most stable family was transferred to a Silicon Graphics Fuel workstation for the next calculation using the Accelrys software package (see below). It was energy-minimized by 500 steps of a steepest descent algorithm with Discover using the consistent-valence force field (cvff) model.

The polyphenol structures were obtain from the Brookhaven Data Bank because these molecules were studied as enzyme substrates. For quercetin we used 1H1I and 1E8W from refs *18* and *19*, respectively. Unfortunately, the structure of quercetin-3-*O*-glucoside was not available so we used the structure of rutin (quercetin-3-*O*-rhamnosyl(1→6)-glucoside): 1RY8 from ref *20*. The quercetin rings were quasi-coplanar with a slight 6° twist around the C2−C1′ bond which connects the exocyclic phenyl B-ring to the rest of the molecule. In the case of quercetin-3-*O*-glucoside, a 32° twist was observed. The polyphenolic molecules and EP were built using the "Accelrys" builder module and then energy-minimized by 500 steps of a steepest descent algorithm with Discover using the consistent-valence force field (cvff) model.

To obtain the putative complex structures from NMR data, molecular modeling was conducted on a Silicon Graphics Fuel workstation using the Accelrys software package. Simulated annealing (SA) and energy

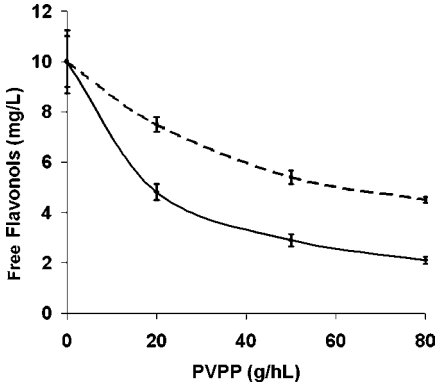

Figure 1. Effects of PVPP on quercetin (solid line) and quercetine-3-*O*-glucoside (dotted line) in dry white wines. Tests were done under conditions resembling those of a winery. Mean values and standard deviations of three independent measurements are presented.

minimization were done with Discover and NMR-Refine using the consistent-valence force field (cvff) model. Interproton distances were obtained from ROESY spectra. Pseudoatoms were used for protons that could not be stereospecifically attributed. Hydrogen bonds between CO−N linkages and phenol groups were also used as distance constraints. SA calculations involved 14 separate phases. The first phase involved 100 steps of randomization and minimization of the starting structure into the steepest descent algorithm. The second phase involved additional minimization into 500 iterations of the conjugate gradient algorithm. Dynamic phases 3−5 involved simulated annealing for 30, 10, and 10 ps, respectively, at 1000 K. Meanwhile, the force constants were increased stepwise up to their full values. Phases 6−10 involved cooling of the molecule from 1000 to 300 K over 10 ps. Phases 11 and 12 involved minimization using 100 steps of the steepest descent algorithm followed by 500 iterations of the conjugate gradient. Finally, the last two minimization phases involved 100 steps of a steepest descent followed by 1500 iterations of a conjugate gradient with a distance-dependent dielectric constant to mimic the solvent effect.

SA calculations were started from 50 initial random structures. We selected final solution structures with the lowest energy, in agreement with NMR experimental constraints. Structural statistics for the converged structures were evaluated in terms of mutual RMSDs and RMSDs between refined structures and their average structure. Various calculations were made: quercetin with three EP, quercetin with EP5, and quercetin-3-*O*-glucoside with EP5. To display the possible interactions in the complexes formed between organic molecules and polyphenols, we used "Protein explorer" (*21*).

RESULTS

To determine the putative prevention of quercetin sedimentation in dry white wines by PVPP, tests were done under conditions resembling those of a winery (**Figure 1**). On the basis of recommended PVPP concentrations in wines (maximum: 80 g/hL) (*14*), quercetin- and quercetin-3-*O*-glucoside-free concentrations were diminished by 79% and 55% respectively. There was a significant difference between quercetin and quercetin-3-*O*-glucoside affinities for PVPP. We therefore studied PVPP interactions with quercetin and quercetin-3-*O*-glucoside in model solutions to understand the differences in affinity observed.

The results of the interaction of quercetin or quercetin-3-*O*-glucoside with PVPP in methanol solutions are shown in **Figure 2**. In agreement with the previous results, the curves clearly show that the association was stronger with aglycone than with its glucoside. Under our experimental conditions, the PVPP molar concentration was unknown, and by using the least-squares fitting technique, we were able to calculate only the apparent binding constants and not the true binding constants.

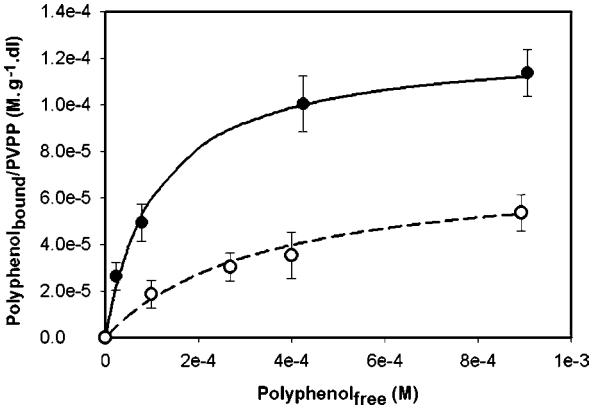

Figure 2. Interaction of quercetin (solid line) or quercetin-3-*O*-glucoside (dotted line) with PVPP in methanol model solutions. Mean values and standard deviations of three independent measurements are presented.

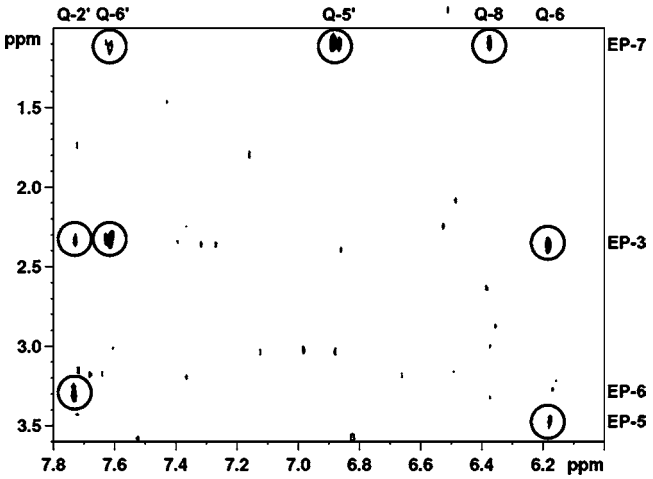

Figure 3. 400 ms ROESY spectrum at 303 K of quercetin and EP mixing according to the molar ratio 1/20. The intermolecular cross-peaks of interest are in circles.

Table 1. Intermolecular ROE's Observed between Polyphenol Protons and Protons of EP[a]

quercetin	1-ethyl-2-pyrrolidinone
2′	3(ww) and 6(w)
5′	7(w)
6′	3(w) and 7(ww)
6	3(ww) and 5(ww)
8	7(ww)
quercetin-3-*O*-glucoside	**1-ethyl-2-pyrrolidinone**
2′	3(ww) and 6(w)
5′	7(ww)
6′	
6	4(ww), 5(ww), and 6(ww)
8	3(ww) and 7(w)

[a] All relative intensities are weak, corresponding to an upper constraint limit of 5.0 Å.

The values obtained were as follows: $K_d = 3.3 \pm 0.6$ g dL^{-1} with $n = 4 \pm 1$ and $K_d = 15 \pm 3$ g dL^{-1} with $n = 3 \pm 1$ for quercetin and quercetin-3-*O*-glucoside, respectively. From these values, we concluded (i) that the association of PVPP with quercetin was 4−5-fold better than that with its glucoside and (ii) that PVPP interacts with the same number of quercetin and quercetin-3-*O*-glucoside molecules. To account for this finding,

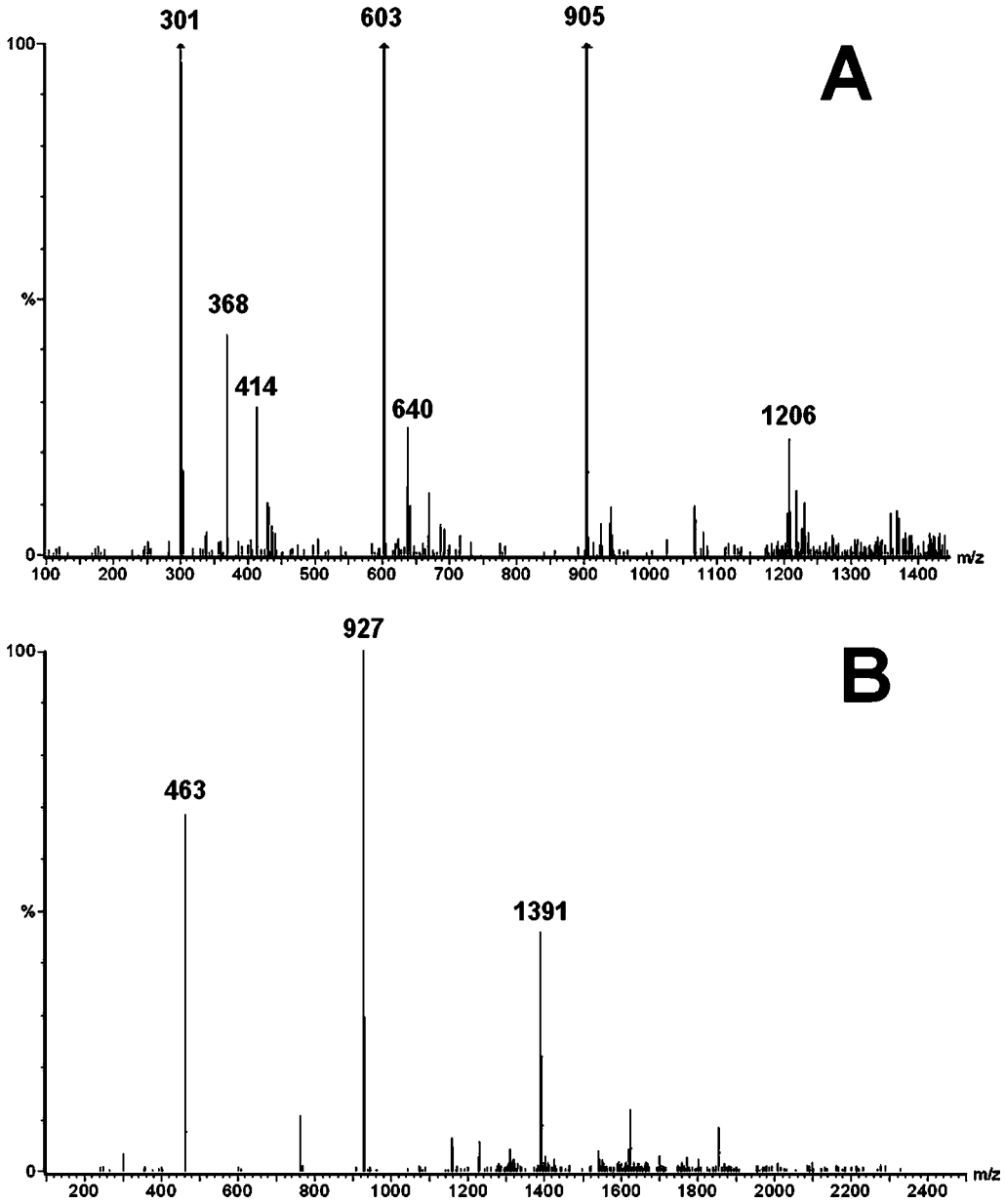

Figure 4. Electrospray mass spectra of the mixtures quercetin–EP (**A**) and quercetin-3-*O*-glucoside–EP (**B**) in the molar ratio 1/10.

we studied interactions at the molecular level. To overcome the problem of the complexity of the PVPP molecule and its water-soluble PVP, we used 1-ethyl-2-pyrrolidinone (EP), which, like PVPP, has a pyrrolidinone ring with an alkyl chain and, thus, has a very simple structure. These studies were carried out by NMR and MS.

The molecule protons were assigned unambiguously by using the software Sparky (*22*) and by using the HMBC sequence. The titration experiments gave their binding constant, determined by fitting the chemical shift variations of polyphenol protons. The values obtained for the dissociation constant were 0.27 ± 0.05 M with $n = 13 \pm 5$ and 0.79 ± 0.09 M with $n = 24 \pm 9$ for quercetin−EP and quercetin-3-*O*-glucoside−EP complexes, respectively. This confirmed the negative role of the glucose moiety in the formation of the complex because a weaker association was observed with quercetin-3-*O*-glucoside than with quercetin. During the titration experiments, the chemical shift variation reached a plateau at the molar ratio polyphenol/EP 1/20 (data not shown). This ratio was therefore used in 2D-NMR. ROESY maps showed the intermolecular cross-peaks between quercetin or quercetin-3-*O*-glucoside and EP molecules (**Figure 3** and **Table 1**) and thus the formation of the complexes between both polyphenols and EP.

The mass spectra are presented in **Figure 4**. Pure methanol solutions of molecules were examined separately. Using the experimental conditions described above, quercetin gave an abundant molecular peak $(M-H)^-$ at *m*/*z* 301 and two weaker peaks for the dimer and trimer molecules $(2M-H)^-$ and $(3M-H)^-$ at *m*/*z* 603 and 905, respectively. Quercetin-3-*O*-glucoside principally gave three peaks: $(M-H)^-$ at *m*/*z* 463, $(2M-H)^-$at *m*/*z* 927, and $(3M-H)^-$ at *m*/*z* 1391, with the latter being weak (data not shown). For the mixture solutions, the polyphenol/EP ratios 1/1 and 1/10 gave the same mass spectra. The spectra had the same abundant peaks due to polyphenols alone. However, with quercetin, molecular complexes with EP were clearly visible (**Figure 4A**). Thus, the relatively intense peaks at *m*/*z* 414, at *m*/*z* 640, and at *m*/*z* 1206 were attributed to the 1:1 complex $(\text{quercetin} + \text{EP} - \text{H})^-$, to the 1:3 complex $(\text{quercetin} + 3\text{EP} - \text{H})^-$, and to the 1:8 complex $(\text{quercetin} + 8\text{EP} - \text{H})^-$. On the contrary, for quercetin-3-*O*-glucoside, these

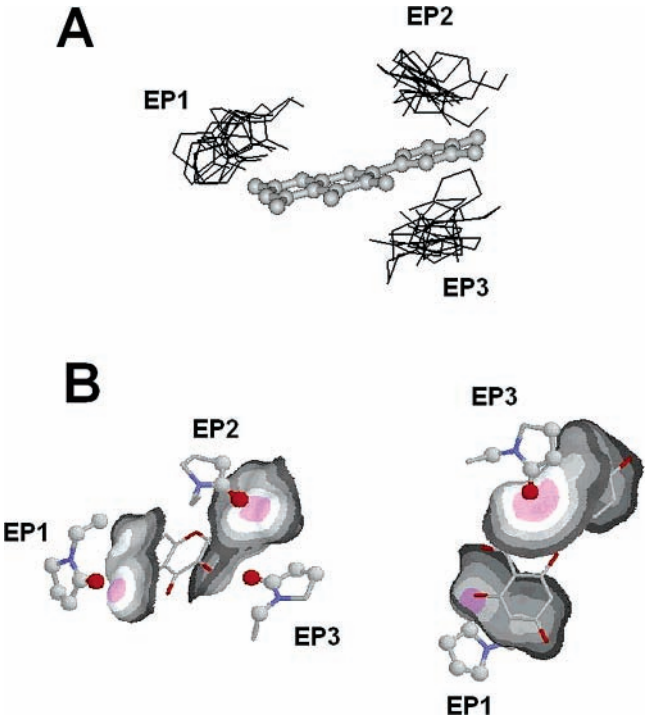

Figure 5. (**A**) Family of nine structures for a putative complex between quercetin and three EP molecules. (**B**) The closest structure to the mean SA structure of this family. Quercetin is represented by its solvent-accessible surface. The magenta regions represent the possible hydrogen bonds, and the pale gray-to-white regions are involved in hydrophobic interactions. For EP species, the atoms within bonding distances are shown as balls-and-sticks.

complexes were not observed. Only quercetin-3-*O*-glucoside and its dimer and trimer were observed (**Figure 4B**).

From the NMR and MS data, we obtained the three-dimensional structure (3D structure) of a possible complex between quercetin and three EP molecules (**Figure 5**). In a first step in the SA protocol, we used only one EP molecule positioned close to the quercetin ring A to explore the conformational space. On the basis of these results, a second EP molecule was added close to quercetin ring B. This second step led to the third step, i.e., placing the third EP molecule close to ring C. These two latter steps were repeated as many times as necessary in order to situate correctly these EP molecules while respecting all intermolecular ROEs (Table 1). Indeed, when a position was false, we obtained large violations of the distance restraints and/or systematic violations of one bond for the molecule majority and/or distortions of the quercetin plane. In the final SA, 50 structures were calculated and 46 low total energy structures respecting NMR restraints were detected. These 46 structures were split into several families on either side of the quercetin plane, with the family populations being close. For example, the family (9 structures) shown in **Figure 5A** had EP1 and EP2 above the plane and EP3 below. **Figure 5B** shows the closest structure to the mean SA structure, where the contact surfaces are colored according to their distances. Quercetin is represented by its solvent-accessible surface (*21*). The magenta regions represent the putative hydrogen bonds, and the pale gray-to-white regions are involved in hydrophobic interactions. For clarity, only the covalent bonds within 7 Å are shown as sticks for all the molecules, and for the EP species, the atoms within bonding distances are shown as balls-and-sticks. These representations clearly show the possible anchoring points of the EP molecules with polyphenol.

These results can be extrapolated to the building of a 3D structure of the complex between both polyphenols and a pentameric structure of PVP (EP5). Molecular modeling of the pentameric structure of PVP showed that the most stable family presented alternate pyrrolidone rings in relation to the alkyl backbone. In this orientation, the angles between two consecutive rings were equal to 105 ± 40° and the distances between the O atoms were almost equal, with a mean value of 5.4 ± 0.7 Å. The alternate pyrrolidone rings are clearly shown in **Figure 6A**. These results are in agreement with a recent report where a trimer structure of PVP was studied (*23*). From these results and those obtained with the complex of quercetin with three EP molecules, we calculated a putative 3D structure of the complex between quercetin and an EP5 molecule with three pyrrolidone rings (**Figure 6**). Very numerous steps were used in the SA protocol where the distance constraints obtained from Table 1 were introduced one by one to avoid large violations of the distance restraints and/or systematic violation of one bond and/or large distortions of the quercetin plane and EP5. In the final SA, 50 structures were calculated and 21 low total energy structures respecting NMR restraints were detected. **Figure 6A** shows the heavy atom superimposition of the EP5 "alkyl" backbone with an RMSD value equal to 0.39 Å. **Figure 6B** shows the weak scattering of EP5 molecules around quercetin when the heavy atoms of quercetin were superimposed (RMSD = 0.05 Å). Interaction with the polyphenol modified the EP5 structure only slightly with angles between two consecutive rings equal to 101 ± 55° and the distances between the O atoms equal to 5.4 ± 1.6 Å. **Figure 6C** shows the closest structure to the mean SA structure, where the contact surfaces are colored according to their distances, as mentioned above. EP5 is represented by its solvent-accessible surface. For quercetin, the atoms within bonding distances are shown as balls-and-sticks (*21*). For clarity, only the covalent bonds within 7 Å are shown as sticks for both molecules.

The same study was performed with the association quercetin-3-*O*-glucoside−EP5. In the final SA, 50 structures were calculated and 16 low total energy structures respecting NMR restraints were detected. **Figure 7** shows a putative 3D structure of the complex. **Figure 7A** shows the heavy atom superimposition of the EP5 "alkyl" backbone with an RMSD value equal to 0.42 Å. **Figure 7B** shows the scattering of EP5 molecules around the polyphenol when its heavy atoms (RMSD = 0.10 Å) were superimposed. **Figure 7C** shows the closest structure to the mean SA structure where the contact surfaces are colored according to their distances, as mentioned above (*21*).

DISCUSSION

The present results show that the association of PVPP with quercetin is 4−5-fold better than that with its glucoside. This is in agreement with previous results where rutin with a sugar moiety (rhamnosylglucoside) was less reactive than quercetin with whey proteins (*11*). The results obtained with the association between polyphenols and EP molecules confirm this better association with the aglycone. Therefore, the hypothesis of the interaction of the synthetic polymers with polyphenols only via H bonds between their CO−N linkages and phenol groups is not sufficient. Indeed, there are five and eight hydroxyl groups in quercetin and quercetin-3-*O*-glucoside monomers, respectively, and thus five and eight potential binding sites. Moreover, mass spectrometry detected polyphenol associations: dimer molecules with 10 and 16 hydroxyl groups and trimer molecules

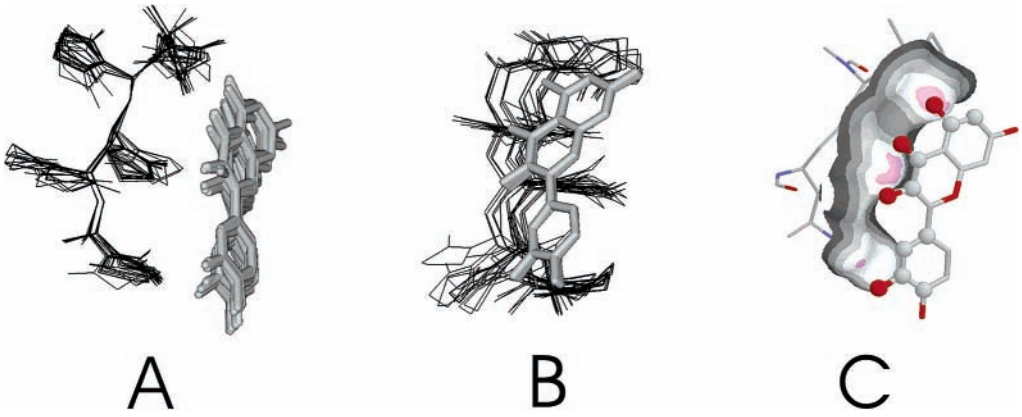

Figure 6. 21 structures of quercetin–EP5 complexes. (**A**) Heavy atom superimposition of the EP5 "alkyl" backbone (RMSD = 0.39 Å). (**B**) Heavy atom superimposition of quercertin (RMSD = 0.05 Å) showing the weak scattering of EP5 molecules. (**C**) The closest structure to the mean SA structure of this family. EP5 is represented by its solvent-accessible surface. For quercetin, the atoms within bonding distances are shown as balls-and-sticks. For both molecules, only the covalent bonds within 7 Å are shown as sticks.

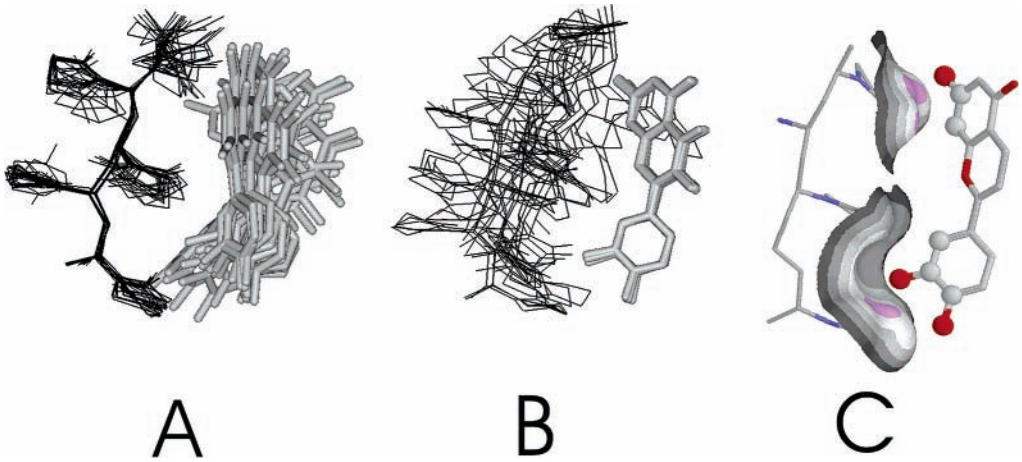

Figure 7. 16 structures of quercetin-3-*O*-glucoside–EP5 complexes. (**A**) Heavy atom superimposition of the EP5 "alkyl" backbone (RMSD = 0.42 Å). (**B**) Heavy atom superimposition of quercetin-3-*O*-glucoside (RMSD = 0.10 Å) showing the scattering of EP5 molecules around the polyphenol. (**C**) The closest structure to the mean SA structure of this family. EP5 is represented by its solvent-accessible surface. For quercetin-3-*O*-glucoside, the atoms within bonding distances are shown as balls-and-sticks. For both molecules, only the covalent bonds within 7 Å are shown as sticks.

with 15 and 24 hydroxyl groups. The mean number *n* of EP molecules associated with quercetin-3-*O*-glucoside (24 ± 9), which was higher than that with quercetin (13 ± 5), might be in agreement with the mean number of potential binding sites present in polyphenols. Thus, the glucose bulk and its hydrophilic character seem to partially prevent interaction with PVPP, suggesting that hydrophobic interactions between the pyrrolidone and phenol rings could play a role.

Our molecular approach confirmed this hypothesis. The quercetin structure allowed a good interaction with PVP because the distance between the hydroxyl groups of the three rings is in accordance with the distance between the three carboxylic functions of the pyrrolidone rings. As clearly shown in **Figure 6C**, the formation of the complex is due to two types of interaction: hydrophobic interaction between the phenolic and pyrrolidinone rings and H bonds between the hydroxyl functions and the CO−N linkages. Interestingly, the pyrrolidone ring and the proline residues in the protein were similar in structure; these findings are in agreement with those observed in polyphenol−protein complexes (*5*). Moreover, in the quercetin−PVP complex, conformational mutual adaptation, thanks to the high flexibility of PVP, allowed them to adopt steric complementarity and to create additional van der Waals bonds with a continuous contact surface. However, in aqueous medium and with the fast equilibrium between free and bound molecules (*24*), it is particularly tricky to assess van der Waals bonds.

On the other hand, in the quercetin-3-*O*-glucoside−PVP complex, the presence of the glucoside moiety in position 3 removed this H bond and forced the polyphenol to present its other side to the PVP (**Figures 6** versus **7**). This has three consequences in addition to the loss of the H bond: (i) the loss of hydrophobic interaction for polyphenol ring C, (ii) a weakening of van der Waals bonds with a discontinuous contact surface, and (iii) a less structured complex with wider scattering of EP5 molecules around the polyphenol (**Figures 6B** versus **7B**). Thus, these molecular data could explain the observation of a weaker complex with PVPP for quercetin-3-*O*-glucoside than for its aglycone.

These conclusions are also in agreement with the NMR and MS results observed with EP. The intermolecular ROEs with EP were observed with both polyphenols, suggesting formation of the complex between the molecules. Moreover, in MS only EP complexes with quercetin were detected. In the gas phase, the external medium (vacuum) is widely considered as being hydrophobic, thus reinforcing the strength of H bonds compared to hydrophobic and van der Waals interactions. In solution, the ionic interaction becomes weaker while the hydrophobic effect becomes greater, whereas the contrary occurs in the gas phase

(*25*). Thus, the H bond alone cannot explain the formation of polyphenol−PVPP complexes. Rather, a range of complementary forces maintain their stability.

In conclusion, this work demonstrates that PVPP preferentially forms complexes with polyphenol aglycones. Therefore, PVPP could be used to prevent quercetin sedimentation. Even though polyphenol concentrations in dry white wines are low, any decrease in free aglycone concentrations will minimize the interactions between proteins and polyphenols, essentially the aglycone forms, which are responsible for haze and precipitates.

ACKNOWLEDGMENT

We are grateful to Dr. Ray Cooke for reading this manuscript.

LITERATURE CITED

(1) Ziemelis, G.; Pickering, J. Precipitation of flavonols in a dry red table wine. *Chem. Ind.* **1969**, *49*, 1781−1782.
(2) Ribereau-Gayon, P. Les composes phénoliques du Raisin et du Vin. *Ann. Physiol. Végét*. **1964,** *2*, 119−147.
(3) Somers, T. C.; Ziemelis, G. Flavonol haze in white wines. *Vitis* **1985**, *24*, 43−50.
(4) Price, S. F.; Breen, P. J.; Valladao, M.; Watson, B. T. Cluster Sun Exposure and Quercetin in Pinot noir Grapes and Wine. *Am. J. Enol. Vitic*. **1995**, *46***,** 187-194.
(5) Haslam, E. Natural Polyphenols (Vegetable Tannins) as drugs: Possible Modes of Action. *J. Nat. Prod*. **1996,** *59*, 205−215 and references cited herein.
(6) Siebert, K. J.; Lynn, P. Y. Effect of Protein-Polyphenol Ratio on the Size of Haze Particles. *J. Am. Soc. Brew. Chem*. **2000**, *58*, 117−123 and references cited therein.
(7) Charlton, A. J.; Baxter, N. J.; Khan, M. L.; Moir, A. J. G.; Haslam, E.; Davies, A. P.; Williamson, M. P. Polyphenol/Peptide Binding and Precipitation. *J. Agric. Food Chem.* **2002**, *50*, 1593−1601 and references cited herein.
(8) Moine-Ledoux, V.; Dubourdieu, D. An invertase fragment for improving the protein stability of dry white wines. *J. Sci. Food Agric.* **1999**, *79*, 537−543.
(9) Richard, T.; Vitrac, X.; Merillon, J. M.; Monti, J. P. Role of peptide primary sequence in polyphenol-protein recognition: An example with neurotensin. *Biochim. Biophys. Acta* **2005,** *1726*, 238−43.
(10) Richard, T.; Lefeuvre, D.; Descendit, A.; Quideau, S.; Monti, J. P. Recognition characters in peptide-polyphenol complex formation. *Biochim. Biophys. Acta*, available online 20 February 2006.
(11) Rawel, H. M.; Rohn, S.; Kroll, J. Influence of a sugar moiety (rhamnosylglucoside) at 3-O position on the reactivity of quercetin with whey proteins. *Int. J. Biol. Macromol.* **2003**, *32*, 109−120.
(12) Pierpoint, W. S. The Extraction of Enzymes from Plant Tissues Rich in Phenolic Compounds. In *Methods in Molecular Biology*; Doonan, S., Ed.; Humana Press Inc.: Totowa, 2004; Vol. 244, pp 65−74 and references cited therein.
(13) Siebert, K. J.; Lynn, P. Y. Comparison of Polyphenol Interactions with Polyvinylpyrrolidone and Haze-Active Protein. *J. Am. Soc. Brew. Chem.* **1998**, *56*, 24−31.
(14) Résolution (5/87); Fiche code OIV Ed 01/2005 II3.4-10.
(15) Baxter, N. J.; Lilley, T. H.; Haslam, E.; Williamson, M. P. Multiple interactions between polyphenols and a salivary proline-rich protein repeat result in complexation and precipitation. *Biochemistry* **1997**, *36*, 5566−5577.
(16) Chang, G.; Guida, W. C.; Still, W. C. An internal coordinate Monte Carlo method for searching conformational space. *J. Am. Chem. Soc*. **1989**, *111*, 4376−4386.
(17) Saunders, M.; Houk, K. N.; Wu, Y. D.; Still, W. C.; Lipton, M.; Chang, G.; Guida, J. Conformations of Cycloheptadecane. A Comparison of Methods for Conformational Searching. *J. Am. Chem. Soc*. **1990**, *112*, 1419−1427.
(18) Steiner, R. A.; Kalk, K. H.; Dijkstra, B. W. Anaerobic enzyme-.substrate structures provide insight into the reaction mechanism of the copper-dependent quercetin 2,3-dioxygenase. *Proc. Natl. Acad. Sci. U.S.A.* **2002**, *99*, 16625−16630.
(19) Walker, E. H.; Pacold, M. E.; Perisic, O.; Stephens, L.; Hawkins, P. T.; Wymann, M. P.; Williams, R. L. Structural determinants of phosphoinositide 3-kinase inhibition by wortmannin, LY294002, quercetin, myricetin, and staurosporine. *Mol. Cell.* **2000**, *6*, 909−919.
(20) Komoto, J.; Yamada, T.; Watanabe, K.; Takusagawa, F. Crystal structure of human prostaglandin F synthase (AKR1C3). *Biochemistry* **2004**, *43*, 2188−2198.
(21) Martz, E. Protein Explorer: easy yet powerful macromolecular visualization. *Trends Biochem. Sci*. **2002,** *27*, 107−109.
(22) Goddard, T.D.; Kneller, G. *PARKY 3*; University of California, San Francisco.
(23) Bogdanova, S.; Pajeva, I.; Nikolova, P.; Tsakovska, I.; Muller, B. Interactions of poly(vinylpyrrolidone) with ibuprofen and naproxen: experimental and modeling studies. *Pharm. Res.* **2005**, *22*, 806−815.
(24) Murray, N. J.; Williamson, M. P.; Lilley, T. H.; Haslam, E. Study of the interaction between salivary proline-rich proteins and a polyphenol by 1H-NMR spectroscopy. *Eur. J. Biochem.* **1994**, *219*, 923−935.
(25) Penn, S. G.; He, F.; Green, M. K.; Lebrilla, C. B. The use of heated capillary dissociation and collision-induced dissociation to determine the strength of noncovalent bonding interactions in gas-phase peptide-cyclodextrin complexes. *J. Am. Soc. Mass Spectrom.* **1997**, *8*, 244−252.

Received for review February 13, 2006. Revised manuscript received April 11, 2006. Accepted April 12, 2006. The authors thank the "Conseil Régional d′Aquitaine" for financial support.

JF060427A